

# Polymerization of styrene in anionic microemulsion with high monomer content

Xiangling Xu\*, Zhicheng Zhang, Hongkai Wu, Xuewu Ge and Manwei Zhang

Department of Applied Chemistry, University of Science and Technology of China,  
 Hefei 230026, People's Republic of China

(Received 27 January 1997; revised 24 March 1997; accepted 12 May 1997)

The styrene microemulsion with high monomer content was stabilized by an emulsifier with a Y structure. When the microemulsion polymerization was initiated with azobisisobutyronitrile (AIBN) or benzoyl peroxide (BPO), a plateau of polymerization rate was observed at low initiator and high monomer content. In the plateau, it was the number of growing polymer particles that was kept constant, instead of the number of total polymer particles. The length of the plateau of  $R_p$  is reduced with the increase of initiator concentration and the decrease of monomer concentration, and even disappears at very low monomer content and very high initiator concentration. Under the similar condition, the polymerization rate and the molecular weight of polystyrene produced are both lower when the initiator is BPO. © 1998 Elsevier Science Ltd. All rights reserved.

(Keywords: microemulsion polymerization; plateau of polymerization rate; styrene polymerization)

## INTRODUCTION

Since Stoffer and Bone published their first paper on microemulsion polymerization in 1980, great development has been made in this new branch of emulsion polymerization. Styrene, as a typical monomer being sparingly soluble in water, was widely investigated in different microemulsion polymerization systems.

Emulsifier sodium dodecyl sulfate (SDS) was the unique anionic emulsifier used in microemulsion polymerization of styrene. However, only with the help of coemulsifier, such as n-pentanol, can SDS form transparent microemulsion. The polymerization kinetics in this system were studied with different methods<sup>1–4</sup>. It was found that there was no constant rate period and no gel effect during polymerization. The number of polymer particles kept increasing with conversion<sup>5</sup>. The mixed micelles composed of SDS, n-pentanol and styrene, were the continuous nucleation places. A mathematical model was proposed by Guo *et al.* to simulate the polymerization<sup>6</sup>.

Cationic emulsifiers, such as cetyltrimethylammonium bromide (CTAB), tetradecyltrimethylammonium bromide (TTAB), and octadecyltrimethylammonium chloride (OTAC), may stabilize styrene microemulsion without the help of cosurfactant. The polymerization kinetics and polymerization mechanism<sup>7–9</sup> in this ternary system were similar to that in microemulsions stabilized with SDS.

A mixture of nonionic emulsifier, ethoxylated nonylphenol with different moles of ethyl oxide (OP), was also used to produce styrene microemulsion for polymerization. In this system, Larpent and Tadros<sup>10</sup> produced nanoparticles of PSt with diameters of 18–24 nm.

In all the above microemulsions for polymerization, the monomer content is much lower and the emulsifier content is much higher than that in an emulsion for polymerization. In this paper, a specially designed emulsifier with a Y structure, in other words, with a branch in the lipophilic

head, was chosen to form the microemulsion of styrene. In this way, the monomer content in microemulsion polymerization could be increased up to 20 wt.%. The polymerization kinetics of styrene in this new system was studied with different oil-soluble initiators, azobisisobutyronitrile (AIBN) and benzoyl peroxide (BPO).

## EXPERIMENTAL

### Materials

Styrene (St) was distilled at 10 mmHg to remove inhibitor and stored at  $-10^{\circ}\text{C}$ . AIBN and BPO were used without further purification. Sodium 12-hexinoyloxy-9-octadecenate (SHOA) was synthesized following the method described in ref. <sup>11</sup>.

### Phase diagram of microemulsion

The clear regions of microemulsions consisting of St, SHOA and water were determined at room temperature (*ca.*  $25^{\circ}\text{C}$ ). St was dropped into the aqueous phase with different SHOA concentrations. The turbidity of the mixture was adapted as the criterion for the formation of microemulsion. The stable microemulsion regions after polymerization were also established by polymerizing the systems with gamma rays ( $40\text{ Gy min}^{-1}$ ) at room temperature.

### Polymerization

Polymerization of St was carried out in a glass dilatometer. After degassing twice with water pump to remove oxygen, the microemulsion was introduced directly into a dilatometer. The change of liquid level in the capillary of the dilatometer was monitored as a function of time. The fractional conversion of St was calculated from the volume change. The rate of polymerization was then derived by differentiation.

### Molecular weight of polystyrene

The polymerized microemulsions were precipitated in a

\* To whom correspondence should be addressed

large quantity of methanol. The resulted polymer was dissolved in toluene, and then reprecipitated with methanol to remove emulsifier completely. After that, the polymer was dried under vacuum. The molecular weight of polystyrene ( $M_n$ ) was measured with an Ubbelohde capillary viscometer, in toluene solution at 25°C:  $[\eta] = 1.34 \times 10^{-2} M_n^{0.71} \text{ ml g}^{-1}$ .

RESULTS

The phase diagram of the microemulsion

In the previous microemulsions of St, which were stabilized with SDS<sup>12</sup>, OP<sup>10</sup>, OTAC or TTAB<sup>9</sup>, the efficiency of surfactant was much lower, and the highest St content less than 10 wt.%. In this paper, the Y-shaped anionic surfactant SHOA, which has a branch in the lipophilic head was chosen to form St microemulsion. In Figure 1, the stable microemulsion regions before and after polymerization are presented. It is obvious that the stable region is much bigger than the previous systems stabilized with SDS<sup>12</sup>, OP<sup>10</sup>, OTAC or TTAB<sup>9</sup>.

The microemulsion consisting of 16.7% St, 15.0% SHOA, 68.3% H<sub>2</sub>O, was selected to study the polymerization kinetics.

Polymerization initiated with AIBN

*Effect of AIBN concentration.* Polymerization rates at different AIBN concentrations were plotted against the conversion in Figure 2. There was an apparent plateau of polymerization rate at low AIBN concentration, but the length of the plateau was reduced with the increase of

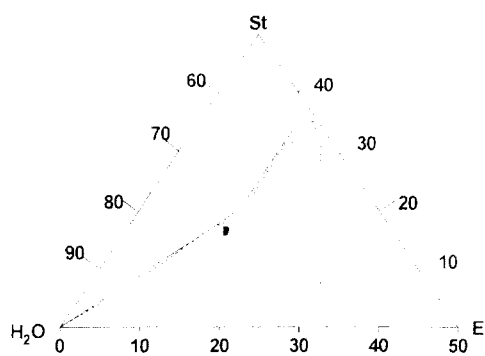


Figure 1 The partial phase diagram of styrene microemulsion stabilized with SHOA. The area enclosed with a solid line is the stable region before polymerization, and the area enclosed with a dashed line is the stable region after polymerization

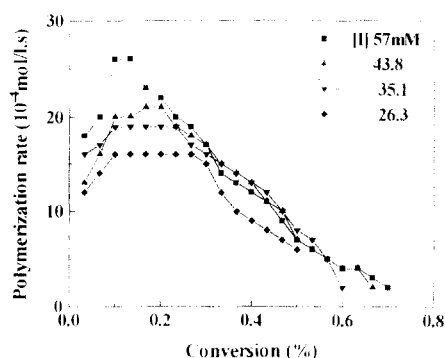


Figure 2 Polymerization rate versus conversion at different AIBN concentrations, St, 16.7 wt.%; E, 15.0 wt.%; pH, 9; T, 333 K

AIBN concentration and even disappeared at high AIBN concentration. It is shown in Figure 3 that  $R_p \propto [AIBN]^{0.38}$ ,  $M_n \propto [AIBN]^{-0.53}$ .

*Effect of emulsifier concentration.* It was shown in Figures 4 and 5 that the polymerization rate increased with the emulsifier content. The plateau of polymerization rate was not so obvious:  $R_p \propto [E]^{0.38}$ ,  $M_n \propto [E]^{-0.39}$ .

*Effect of St concentration.* As shown in Figure 6, the plateau of  $R_p$  was prolonged with the increase of St concentration. The plateau even disappeared at low monomer concentration. The polymerization rate and

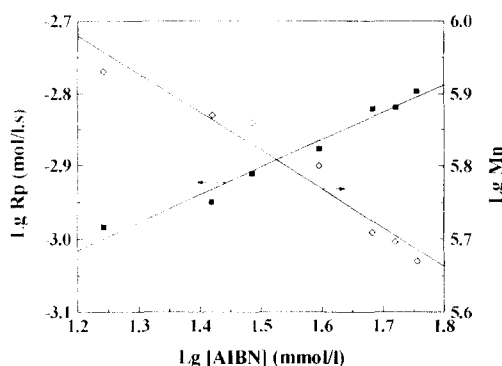


Figure 3 Effect of AIBN concentration on polymerization. St, 16.7 wt.%; E, 15.0 wt.%; pH, 9; T, 333 K

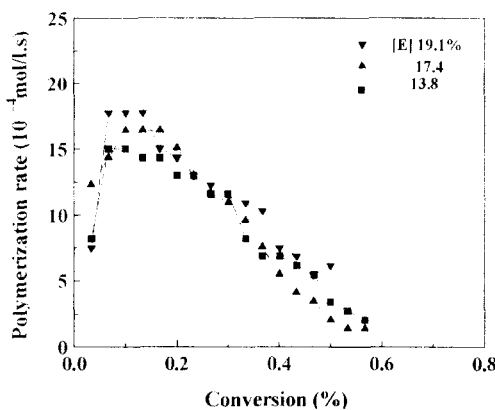


Figure 4 Polymerization rate versus conversion at different emulsifier contents. [AIBN], 19 mmol l<sup>-1</sup>; St, 15 wt.%; pH, 9; T, 333 K

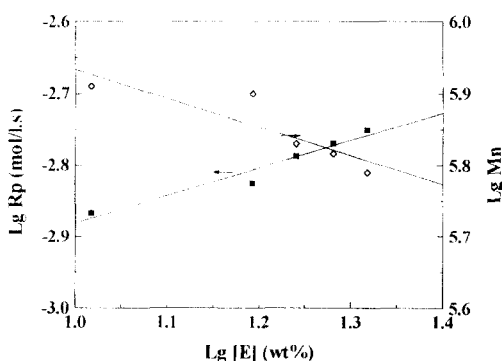


Figure 5 Effect of emulsifier content on polymerization. [AIBN], 19 mmol l<sup>-1</sup>; St, 15 wt.%; pH, 9; T, 333 K

the molecular weight of polymer increased with St concentration:  $R_p \propto [St]^{0.96}$ ,  $M_n \propto [St]^{1.48}$  (Figure 7).

**Polymerization initiated with BPO**

*Effect of BPO concentration.* Quite out of expectation, there was a peak of polymerization rate when BPO concentration was about  $0.011 \text{ mol l}^{-1}$ , as shown in Figure 8. But the curve of molecular weight versus BPO concentration had no peak. The power of  $M_n$  to BPO concentration was  $-0.76$ .

*Effect of emulsifier concentration.* As in polymerization initiated with AIBN, the polymerization rate was raised and the molecular weight of polymer was lowered with the increase of the emulsifier concentration:  $R_p \propto [E]^{1.88}$ ,  $M_n \propto [E]^{-0.57}$  (Figure 9). The powers of  $R_p$  and  $M_n$  to emulsifier concentration were both higher than in the AIBN case.

*Effect of St concentration.* When the initiator was BPO, the effect of monomer concentration on polymerization showed the same tendency as when the initiator was AIBN. As depicted in Figure 10,  $R_p \propto [St]^{2.63}$ ,  $M_n \propto [St]^{0.99}$ . The powers were also different from that when the initiator was AIBN.

**DISCUSSION**

*Cause of the plateau of polymerization rate*

For microemulsion polymerization, the monomer droplets are of the same order of micelles. So monomer droplets may compete with micelles to form polymerization loci. It is believed that there is no obvious difference

between these two reaction loci. This is quite different from that in emulsion polymerization. Therefore, the mechanism for the plateau of polymerization rate is sure to be different from that for emulsion polymerization.

The emulsifier content in microemulsion polymerization is much higher than that in emulsion polymerization, so the micelles in microemulsion polymerization remain in the system throughout the polymerization. Then the nucleation process may continue to very high conversion, and the number of polymer particles keeps on accumulating. This has been really observed in several systems<sup>5,13,14</sup>.

As mentioned above, at low conversion, the number of microdroplets and micelles is great, and almost all radicals are used to initiate the microdroplets to form new polymerization loci. Therefore, once the growing polymer

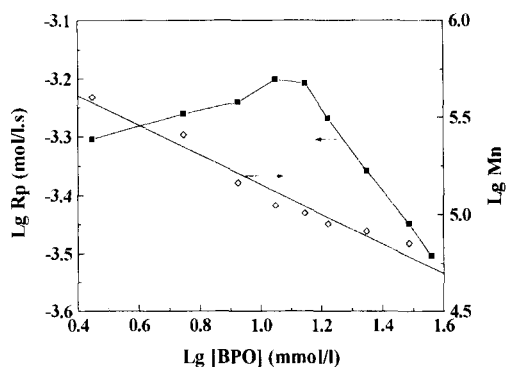


**Figure 8** Effect of BPO concentration on polymerization. St, 16.7 wt.%; E, 15.6 wt.%; pH, 9; T, 333 K

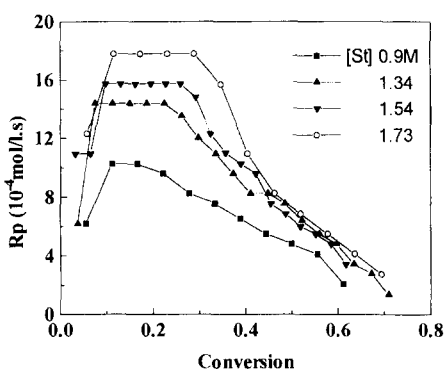


**Figure 6** Polymerization rate versus conversion at different monomer concentration. [AIBN],  $31 \text{ mmol l}^{-1}$ ; E, 15.2 wt.%; pH, 9; T, 333 K

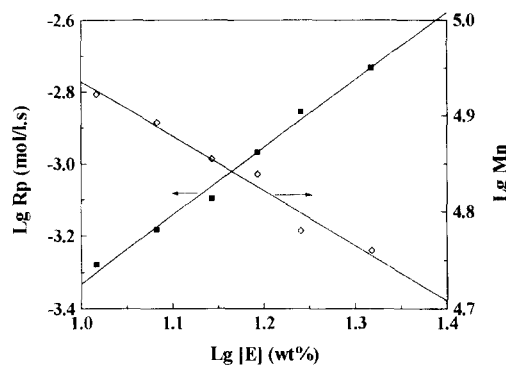


**Figure 9** Effect of emulsifier concentration on polymerization. [BPO],  $16.3 \text{ mmol l}^{-1}$ ; St, 16.7 wt.%; pH, 9; T, 333 K

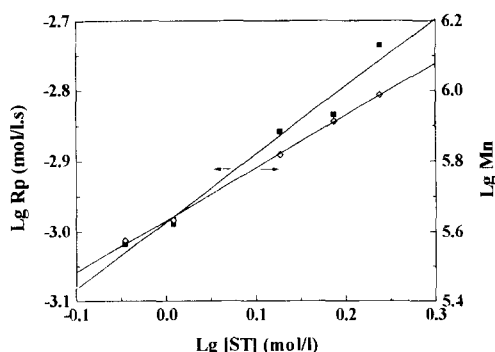


**Figure 7** Effect of St concentration on polymerization. [AIBN],  $31 \text{ mmol l}^{-1}$ ; E, 15.2 wt.%; pH, 9; T, 333 K

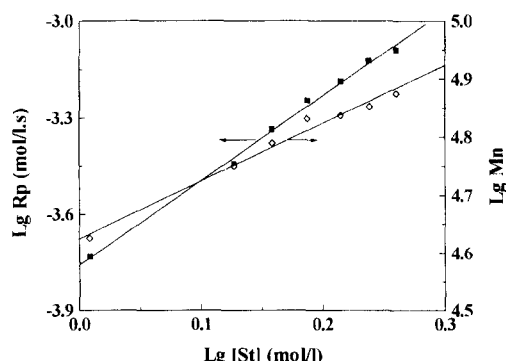


**Figure 10** Effect of St concentration on polymerization. [BPO],  $22.7 \text{ mmol l}^{-1}$ ; E, 15.6 wt.%; pH, 9; T, 333 K

particle is initiated, there will be little probability for them to be terminated with the second radical. The rate of generating new growing particles is much higher than the terminating rate of growing particles. Because the growing particles may terminate through a monoradical mechanism (growing radicals transferring to the lipophile head of emulsifier), with the accumulation of growing particles, the terminating rate is sure to increase. When the terminating rate equals the nucleating rate, the number of growing polymer particles will acquire a balance value. Now if the polymerization loci (growing polymer particles) are still saturated with monomer, the plateau of polymerization rate is sure to appear. So we assume that it is the number of growing polymer particles being kept constant in the plateau, instead of the number of total polymer particles.

Based on the above inference, it is easy to imagine that the length of the plateau depended on the number of growing polymer particles and the remained monomer concentration at the beginning of the plateau. In microemulsion polymerization, monomer diffusion is fast enough to maintain thermodynamic equilibrium. Then, if the number of growing particles is smaller and the monomer concentration is higher, the plateau will appear for wider conversion; otherwise, the plateau will shorten and even disappear. This is just the reason for the results observed in this paper: the length of plateau of  $R_p$  is reduced with the increase of initiator concentration and the decrease of monomer concentration, and even disappears at very low monomer content and very high initiator concentration. It can also answer why the plateau of polymerization rate is scarcely observed in the previous microemulsion polymerization system: because the monomer content in those systems is too low.

#### Discussion of polymerization kinetics

The effect of initiator concentration and monomer concentration on polymerization is similar to the polymerization kinetics initiated with KPS or gamma rays<sup>15</sup>. However, the effect of emulsifier content is obviously different depending on what kind of initiator is adapted, oil soluble or water soluble.

In this case, the initiators are oil soluble, so before polymerization they mainly distribute in the micelles or the microdroplets of monomer. The two decomposed radicals in a same micelle or microdroplet tend to couple rapidly, unless one of them diffuses out or reacts with emulsifier. For example, through adding to the double bond or abstracting the allylic hydrogen in the lipophilic head of the emulsifier. Only when there is only one radical left in the micelle or microdroplet can they be initiated to polymerize. Increase of emulsifier concentration improved the reaction probability of radical with emulsifier concentration. So the initiation efficiency is enhanced with the increase of emulsifier. It further leads to the increase of polymerization rate and the decrease of molecular weight.

Even for oil-soluble initiators, there is still a little difference between AIBN and BPO. When the initiator is BPO, the overall polymerization rate and molecular weight of polymers are a little lower. In expression of polymeriza-

tion kinetics, it is clear that the power of emulsifier and monomer content to  $R_p$  is much higher for BPO than that for AIBN. This may be caused by the fact that the BPO concentration, adapted in *Figures 9 and 10*, is higher than the BPO concentration corresponding to the peak of  $R_p$  in *Figure 8*. Increase of emulsifier and St content in the system leads to the dilution of BPO concentration in polymer particles, and further to the increase of  $R_p$ .

The difference between AIBN and BPO may have some relation with their reactivity in hydrogen abstraction. For BPO, the benzoyloxy radical is much more reactive. So the benzoyloxy radicals produced in the emulsifier layer are more easily able to abstract the allylic hydrogen in the lipophile head of the emulsifier, and to form stable allylic radicals. It is difficult for the allylic radicals to initiate monomer polymerization. So only the benzoyloxy radicals produced in the core of the monomer droplets can initiate polymerization. So when the microemulsion polymerization is initiated with BPO, the real initiation loci may be the core of the monomer droplets. On the other hand, the 2-cyano-2-propyl radical from AIBN is less reactive in hydrogen abstraction. In consideration of the small size of monomer droplets, only when one of the two radicals from AIBN diffuses out of the monomer droplets can the monomer droplets be initiated to polymerize. Therefore the polymerization tends to be initiated in the emulsifier layer when the microemulsion polymerization is initiated with AIBN. In fact, the above conclusions are in good agreement with the experimental results reported by Capek<sup>16</sup>.

However, the peak of  $R_p$  in *Figure 8* is still difficult to understand, and is left to further study.

#### REFERENCES

1. Feng, L. and Ng, K., *Macromolecules*, 1990, **23**, 1048.
2. Holdcroft, S. and Guillet, E.L., *J. Polym. Sci. Part A: Polym. Chem.*, 1990, **28**, 1823.
3. Zhang, Z.C., Xu, X.L., Wu, X. and Zhang, M.W., *J. China Univ. Sci. Technol.*, 1995, **25**, 64.
1. Guo, J.S., El-Aasser, M.S. and Vanderhoff, J.W., *J. Polym. Sci. Part A: Polym. Chem.*, 1990, **27**, 691.
5. Guo, J.S., Sudol, E.D., Vanderhoff, J.W. and El-Aasser, M.S., *J. Polym. Sci. Part A: Polym. Chem.*, 1992, **30**, 691.
6. Guo, J.S., Sudol, E.D., Vanderhoff, J.W. and El-Aasser, M.S., *J. Polym. Sci. Part A: Polym. Chem.*, 1992, **30**, 703.
7. Ferrick, M.R., Murtagh, J. and Thomas, J.K., *Macromolecules*, 1989, **22**, 1515.
8. Puig, J.E., Corona, S. and Maldonado, A., *J. Colloid Interface Sci.*, 1990, **137**, 308.
9. Gan, L.M., Chew, C.H., Lee, K.C. and Ng, S.C., *Polymer*, 1994, **35**, 2659.
10. Larpent, C. and Tadros, T.F., *Colloid Polym. Sci.*, 1991, **269**, 1171.
11. Xu, X.L., Fei, B., Zhang, Z.C. and Zhang, M.W., *J. Polym. Sci. Part A: Polym. Chem.*, 1996, **34**, 1657.
12. Tang, H.I., Johnson, P.L. and Gulari, E., *Polymer*, 1984, **25**, 1357.
13. Gan, L.M., Lee, K.C., Chew, C.H., Tok, E.S. and Ng, S.C., *J. Polym. Sci. Polym. Chem. ed.*, 1995, **33**, 1161.
14. Belger, F., Murthy, A.K., Pla, F. and Kaler, E.W., *Macromolecules*, 1994, **27**, 2559.
15. Xu, X.L., Ge, X.W., Zhang, Z.C., Zhang, M.W., *Radiat. Phys. Chem.*, 1997, **49**, 469.
16. Potisk, P., Vaskova, V., Capek, I. and Klimova, M., *Angew. Makromol. Chem.*, 1996, **236**, 43.